THE

PHYSICAL REVIEW

*A journal of experimental and theoretical physics established by E. L. Nichols in 1893*

SECOND SERIES, VOL. **183**, NO. 2 10 JULY 1969

# Spectra of Hydrogenated Calcium Fluoride Containing Rare-Earth Ions

G. D. JONES,* S. PELED, S. ROSENWAKS, AND S. YATSIV
*Department of Physics, Hebrew University of Jerusalem, Jerusalem, Israel*

(Received 17 December 1968)

Hydrogenation of calcium fluoride containing rare-earth impurities results in the settlement of H$^-$ ions in various lattice positions. The electronic spectra of the rare-earth (RE) impurity ions, infrared absorption due to localized vibration of the H$^-$ ions, vibronic spectra of RE$^{3+}$+H$^-$ ion pairs, and the electron-spin-resonance (ESR) spectra of these pairs are mutually consistent in yielding the position and symmetry of the H$^-$ sites in the lattice. The location of the H$^-$ ions depends on the thermal treatment during and after the hydrogenation. This is observed by reversible and irreversible changes in the various spectra. Spectral changes due to isotopic substitution of H$^-$ by D$^-$ are described and analyzed.

## I. INTRODUCTION

NEGATIVE hydrogen ions can be incorporated into pure calcium fluoride in high concentration.[1] The hydride ion substitutes for the fluoride ion in a regular lattice site of tetrahedral symmetry [Fig. 1(a)]. The crystals show strong infrared absorption due to localized modes of the hydride ion.

In calcium fluoride doped with trivalent ions, the hydride ion can serve as a charge compensator for the impurity ions. In this role it replaces the corresponding fluoride ions in interstitial lattice sites. Since the attainable concentration of hydride ion is relatively high, and due to the electrostatic affinity of the H$^-$ and RE$^{3+}$ ions, one can study the formation of RE$^{3+}$+H$^-$ ion pairs in hydrogenated CaF$_2$ crystals even at low impurity concentrations (0.01%). The studies of such pairs, as well as of isolated hydride and of cluster hydride sites, yield information on the mechanism and stability of various charge-compensation arrangements in the lattice.

There are many ways in which the impurity RE ions can be charge compensated in CaF$_2$. This is reflected in the complexity of the optical and ESR spectra of these ions in the crystal. Each site yields its characteristic spectrum which generally does not overlap the "signature" spectrum of other sites. Weber and Bierig[2] give a summary of the various charge-compensation mechanisms determined by ESR methods. Numerous studies have been made on the optical spectra.[3]

Some of the trivalent RE ions are found to have cubic symmetry characteristics of the substituted Ca$^{2+}$ ion. In these cases it is supposed that charge compensation is not achieved locally and that any charge-compensating ion is remote from the RE ion. These cubic symmetry sites are found to occur more frequently for ions in the latter part of the $4f^n$ series.[2]

A common form of charge compensation is provided by interstitial fluoride ions in an empty fluorine cell[4] adjacent to the trivalent RE ion. The latter is found in a tetragonal ($C_{4v}$) site, with symmetry axes along the $\langle 100\rangle$ crystallographic directions.

Another form of charge compensation[5,6] involves an interstitial fluoride ion in a second-nearest-neighbor fluorine cube producing a trigonal ($C_{3v}$) site symmetry aligned along the $\langle 111\rangle$ crystallographic directions. Many other arrangements of charge compensation by single

---

[*] Permanent address: Department of Physics, University of Canterbury, Christchurch, New Zealand.

[1] R. J. Elliott, W. Hayes, G. D. Jones, H. Macdonald, and C. T. Sennett, Proc. Roy. Soc. (London) **A289**, 1 (1965).

[2] M. J. Weber and R. W. Bierig, Phys. Rev. **134**, 1492 (1964).

[3] P. P. Feofilov, Opt. i Spektroskopiya **6**, 234 (1959) [English transl.: Opt. Spectry. (USSR) **6**, 150 (1959)]; A. A. Kalyanskii, V. N. Medvedev, and P. P. Feofilov, Opt. i Spektroskopiya **14**, 664 (1963) [English transl.: Opt. Spectry. (USSR) **14**, 351 (1963)]; Yu K. Voron'ko, A. A. Kaminskii, and V. V. Osiko, Zh. Eksperim. i Teor. Fiz. **49**, 420 (1965); **49**, 724 (1965) [English transls.: Soviet Phys.—JETP **22**, 295 (1966); **22**, 501 (1966)]; Z. J. Kiss, J. Chem. Phys. **38**, 1476 (1963); J. Makovsky, *ibid.* **46**, 390 (1967); J. Kirton and S. D. McLaughlan, Phys. Rev. **155**, 279 (1967); I. V. Stepanov and P. P. Feofilov, Dokl. Adak. Nauk SSSR **4**, 615 (1957) [English transl.: Soviet Phys.—Doklady **1**, 350 (1960)].

[4] J. Sierro, Helv. Phys. Acta **36**, 505 (1963).

[5] J. Sierro, Phys. Letters **4**, 178 (1963).

[6] U. Ranon and A. Yaniv, Phys. Letters **9**, 17 (1964).

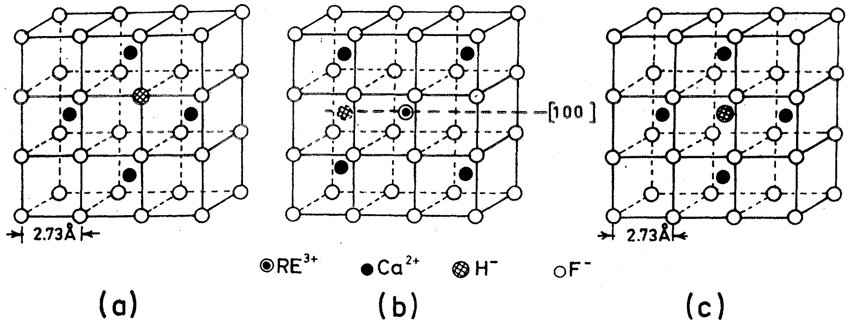

FIG. 1. Schematic representation of the (hydrogenated) calcium-fluoride lattice showing the axial- and cubic-site hydride-ion centers: (a) pure calcium fluoride, (b) the axial-site center, and (c) the cubic-site center.

or multiple fluoride ions at more distant interstitial positions can be visualized.[7]

When oxygen is present in the crystals, it usually forms a divalent $O^{2-}$ ion, replacing a fluorine in one of the eight corner points around the trivalent RE ion.[5,8]

When calcium-fluoride crystals containing RE ions are hydrogenated, it is expected that the hydride ions introduced will also partake in many of these charge-compensation arrangements. In particular, it is expected that a stable RE-hydride ion pair will be formed corresponding to the charge compensation of a trivalent RE ion by a hydride ion in an adjacent empty fluorine cell. Such an ion pair appears strongly in crystals that are rapidly quenched following hydrogenation. This ion pair forms a particularly simple and well-characterized entity amenable to detailed experimental and theoretical investigation, and its study forms a principal part of this paper.

This and other hydrogenic sites may be investigated by the following techniques.

### Infrared Absorption

The hydride-ion impurity gives rise to localized modes which are observed by their infrared absorption. The frequencies and the number of transitions in a particular lattice site are characteristic of the force constants and of the symmetry of the site. Anharmonic effects in the crystal permit the observation of absorption at the harmonic frequencies of the fundamental transitions. The number of harmonic transitions is helpful in determining the exact site symmetry for the hydride ion.

### Electronic and Vibronic Spectra

The absorption and fluorescence spectra of RE ions in crystals consist of sharp lines due to transitions between electronic levels of the $4f^n$ configuration. The coupling of a RE ion to an adjacent hydride ion manifests itself in several ways: (1) by the appearance of new electronic lines due to the change environment of the RE ion caused by the presence of an adjacent hydride ion, (2) by a small, but definite, isotope shift in the frequencies of the new electronic transitions when deuterium is substituted for hydrogen, and (3) by the occurrence of vibronic transitions accompanying the new "parent" electronic transitions and separated from them by the frequencies of the hydride-ion localized modes.

### Irradiation and Thermal Treatments

The electronic and vibronic spectra of hydrogenic site RE ions undergo marked changes following irradiation of the crystal by uv or x radiation. Some of these changes are reversible upon warming the crystal, while others represent a permanent change in which the hydrogen impurity moves to new stable positions. In some cases, marked changes in the electronic transitions of the RE ion are observed which are not accompanied by corresponding alterations of the infrared spectrum of the adjacent hydride ion.

### ESR

ESR is a powerful tool for determining the site symmetry and the crystalline environment of paramagnetic ions. RE ions close to hydride ions are often distinguished by a characteristic thermal behavior and by the slight change in the crystal-field parameters upon substituting deuterium for hydrogen.

Paramagnetic centers in the hydrogenated crystals can also be generated by conversion of the hydride ion to neutral hydrogen atoms through x or uv irradiation. If the irradiation is at low temperature, the hydrogen remains in the same lattice site. The paramagnetic hydrogen atoms can be examined by their ESR spectra, but frequently the desired spectrum is swamped by the stronger absorption of hydrogen atoms unperturbed by adjacent RE ions. In favorable cases, this method yields useful data.

In this paper we give a description and analysis of the hydride ion in two interstitial positions in the calcium-fluoride lattice. In both cases, the hydride ion is a charge compensator for the trivalent RE ions and is only observed in crystals containing RE ions.

Hydrogenation techniques, infrared absorption measurements, electronic and vibronic measurements, and

---

[7] V. V. Osiko, Fiz. Tverd. Tela 7, 1294 (1965) [English transl.: Soviet Phys.—Solid State 7, 1047 (1965)].

[8] J. Sierro, J. Chem. Phys. 34, 2183 (1961).

the results of irradiation and thermal treatments on the spectra are described. The results of ESR investigations will be quoted, but details will be published separately. A preliminary account of this work was presented at the International Conference on Localized Excitations in Solids at Irvine, California, 1967.[9] New results on the electronic and vibronic spectra and, particularly, on the thermal and irradiation changes in the spectra are reported here for the first time.

## II. EXPERIMENTAL TECHNIQUES

The RE-doped calcium fluoride crystals used in these investigations were grown by the Stockbarger method from synthetic calcium fluoride and RE fluorides. Oxygen was removed from the starting material by the use of lead fluoride as a scavenger.

The crystals were first heated under high vacuum at 500°C in the presence of aluminium metal in a quartz tube. Hydrogen or deuterium gas was then introduced at 1-atm pressure, and the temperature was raised to 800–900°C for periods of up to 40 h. This method of introducing hydrogen and deuterium was first applied to calcium fluoride by Hall and Schumacher.[10,11] Rapid quenching of the crystals was achieved by pulling the crystals out of the furnace into room temperature in about 1 min.[4]

Infrared measurements were made in the 4000–200-$\text{cm}^{-1}$ range with a Perkin-Elmer 621 infrared spectrophotometer. Low-temperature spectra were obtained with a metal Dewar; the crystals were cooled by thermal contact with a copper block and reached a temperature somewhat higher than that of the refrigerant. The actual temperature of the crystals was monitored by recording the frequency of the tetrahedral-site-hydride local-mode line at 965.6 $\text{cm}^{-1}$ at 20°K or of its harmonics.[1]

The fluorescence spectra of the crystals containing gadolinium were recorded both photographically and photoelectrically on a Bausch and Lomb two-meter dual-grating spectrograph. The spectra were excited by a Philips 500-W directed-radiation high-pressure mercury lamp. Use was made of a rotating chopper filtering system to completely eliminate any exciting radiation from the fluorescence spectrograms.[12] Wavelengths of the spectral lines were measured to better than 0.1 Å. Lifetime measurements were made by measuring the intensity of the fluorescence lines as a function of the frequency of rotation of the chopper.

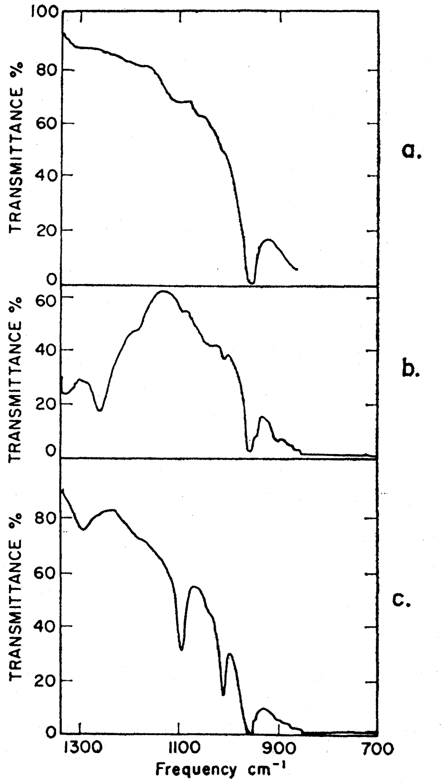

FIG. 2. Low-resolution room-temperature infrared spectrogram of (a) hydrogenated pure calcium fluoride, (b) slowly annealed (20°/h) hydrogenated calcium-fluoride crystal containing gadolinium, and (c) rapidly quenched hydrogenated calcium fluoride containing gadolinium.

## III. THERMAL TREATMENT AND THE HYDRIDE-ION SPECTRA

Calcium fluoride has cubic symmetry (space group $O_h^5$). Each calcium ion is surrounded by eight fluorines at the corners of a cube and every second cube of fluorines is empty (Fig. 1). The point symmetry of the calcium site is cubic $O_h$. The fluorines have four nearest-neighbor calcium ions at the corners of a tetrahedron, and the local site symmetry is tetrahedral $T_d$. The lattice parameter is 5.45 Å.

In calcium-fluoride crystals containing trivalent RE ions, charge compensation is required. The distribution of the RE ions among the different possible charge-compensation arrangements depends on the RE ion concentration and on the thermal treatment during and following the formation of the crystal. In hydrogenated crystals, charge compensation by hydride ions is possible. It is expected, and observed, that marked changes occur in the hydride-ion infrared, electronic, and vibronic spectra following different heat treatments in or after hydrogenation. The effectiveness of the heat treatments in producing changes in the infrared spectra associated with the hydride ion is shown in Fig. 2. The figure represents typical changes in the spectra for crystals subject to extreme cooling rates.

---

[9] G. D. Jones, S. Yatsiv, S. Peled, and S. Rosenwaks, in *Proceedings of the First International Conference on Localized Excitations in Solids*, edited by R. F. Wallis (Plenum Press, Inc., New York, 1968), p. 512.

[10] J. L. Hall and R. T. Schumacher, Phys. Rev. **127**, 1892 (1962).

[11] B. Welber, J. Chem. Phys. **43**, 3015 (1965).

[12] S. Peled, U. El-Hanany, and S. Yatsiv, Rev. Sci. Instr. **37**, 1649 (1966).

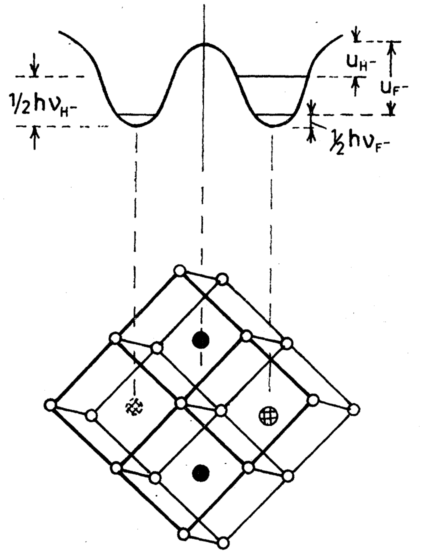

FIG. 3. Schematic representation of the potential barriers for diffusion of interstitial fluoride and hydride ions from one interstitial position to another.

Marked changes were observed in the infrared absorption of a crystal that was stored at room temperature for 2 months. It follows that the migration of hydride ions in the calcium-fluoride lattice is extensive even at room temperature. That this is reasonable may be seen from the following considerations: Ions in interstitial sites move from one position to another and have a certain diffusion rate. The diffusion constant $D$ is equal to $qa^2$, where $q$ is the probability per unit time of motion from one to a neighboring position and $a$ is the distance between adjacent equivalent sites.

The probability $q$ satisfies the relation

$$q=\nu e^{-U/kT},$$

where $\nu$ is the vibration frequency of the interstitial ion and $U$ is the potential barrier that the ion has to climb in its motion between two adjacent wells. Figure 3 describes the situation for the case of an interstitial negative ion in calcium fluoride. The variation of the diffusion constant $D$ and the probability $q$ with the mass of the negative ion can be derived from the last expression as follows: It is plausible to assume that the force constants determining the vibration frequency are not appreciably altered when the fluoride ion is replaced by a hydride ion. The ratio of frequencies $\nu$ of the two ions in the same lattice is, therefore, approximately equal to the inverse square root of their respective reduced masses. The change in frequency affects $q$ through its explicit dependence on $\nu$ and also through the activation energy $U$. As can be seen from Fig. 3, the activation energy is measured from the zero-point level of the vibration. Due to the frequency difference, this level is about four times higher above the minimum of the potential well for a hydride ion than for a fluoride ion. Thus, the diffusion constant changes with the mass of the migrating ion both through the explicit and the implicit dependence on $\nu$. The hydrogenic sites are thus much more affected by thermal treatment than the sites of the unhydrogenated crystals.

Rapid quenching was performed on the crystals with the aim of freezing the hydride interstitial ions in the less stable sites which are well separated from the trivalent RE ions. In crystals treated in this way, such sites are found together with the trivalent RE-hydride ion pair postulated earlier. The spectra of both these sites are strongly reduced when the crystals are annealed and a new complex spectrum of hydride ions in different lattice positions appears. The data pertaining to these new sites is complicated and has not yet been fully analyzed. A preliminary discussion of the behavior of these complex spectra was presented at the Johns Hopkins University Conference on the Optical Properties of Solids.[13] They will not be discussed further here.

The distinction between slow annealing and fast quenching depends on the RE concentration. For RE molar concentrations lower than 0.02%, the simple hydride spectra, characteristic of fast quenching, is obtained even if the crystal is cooled slowly over a period of a few hours. For concentrations greater than 1% molar, the spectra show traces characteristic of annealing no matter how rapidly the crystals are quenched. For intermediate concentrations in the range 0.02–1% molar, both types of spectra are possible. Most of the measurements here were made on 0.05%-concentration crystals.

## IV. INFRARED MEASUREMENTS

Rapid quenching was carried out on crystals of calcium fluoride containing almost all the RE ions as well as yttrium. The infrared absorption spectra of the localized modes of both hydrogen and deuterium in these crystals consists of four lines [Fig. 2(c)]. Two of these lines have frequencies independent of the RE ions. One is the well known 965-cm$^{-1}$ line observed in pure calcium fluoride. The other line has a frequency of 1296 cm$^{-1}$ at room temperature. It occurs only in calcium-fluoride crystals containing RE ions and has its greatest intensity for impurity ions in the second half of the RE series. The remaining two lines have frequencies which vary with the RE ion present and appear always together. All the observed lines are consistent with the hydride ion settling in three lattice sites:

(1) The substitutional position replacing a regular fluoride ion of the calcium-fluoride lattice. This site

---

[13] S. Yatsiv, S. Peled, S. Rosenwaks, and G. D. Jones, in *Proceedings of the Conference on Optical Properties of Ions in Crystals*, edited by H. M. Crosswhite and H. W. Moos (Interscience Publishers, Inc., New York, 1967), p. 409.

has been extensively investigated in pure calcium fluoride and will not be discussed further here.[1]

(2) An interstitial position at the center of an empty fluorine cell well separated from any RE ions [Fig. 1(c)]. This site has cubic $O_h$ symmetry and henceforth will be called the cubic site.

(3) An interstitial position at the center of an empty fluorine cell which is adjacent to a trivalent RE ion in the $\langle 100 \rangle$ direction [Fig. 1(b)]. This has $C_{4v}$ symmetry and will be referred to as the axial site.

The assignment of the observed infrared lines to these sites will now be examined in detail.

### Cubic Site

The single line at 1296 $\text{cm}^{-1}$ at room temperature and 1310 $\text{cm}^{-1}$ at 77°K has a frequency and width only slightly dependent on the RE ion present. The absorption contour is broad and the linewidth is 30 $\text{cm}^{-1}$ at room temperature and 15 $\text{cm}^{-1}$ at 77°K. This line is assigned as due to an interstitial hydride localized vibration at the center of an empty fluorine cell remote from any RE ion. This assignment is of paramount importance for the rest of this work and is based on the following observations:

(a) The transition appears only in crystals where charge compensation is required and is provided by negative ions. Its frequency is almost independent of the RE ion, indicating that it is well separated from them.

(b) The frequency of the transition does not match the separation of a vibronic transition from *any* of the pure electronic lines of gadolinium in crystals containing this ion.

(c) Infrared absorption at the second-harmonic frequency of the fundamental frequency is not observed. A transition to the second excited state is strictly forbidden with inversion symmetry (Fig. 4). However, the low intensity of the fundamental, together with its large width, make the detection of a second harmonic difficult so that this evidence is not entirely reliable.

(d) The site is not stable under annealing thermal treatment. The intensity of the line almost vanishes upon annealing and new absorption lines characteristic of locations close to the RE ions appear as the hydride ion moves to more stable positions, close to the RE ions.

(e) The line is observed only when the RE ion is one of the middle or latter part of the RE series, and its intensity grows along the series. This is consistent with the general behavior of charge compensation in calcium fluoride. It is found that the relative stability of cubic sites of trivalent RE ions increases along the RE series.[2] This stability is a function of the strength of the mutual interaction between the trivalent ion and its charge compensation, and the intensity of the hydrogenic cubic-site line will follow that of the cubic RE ion sites.

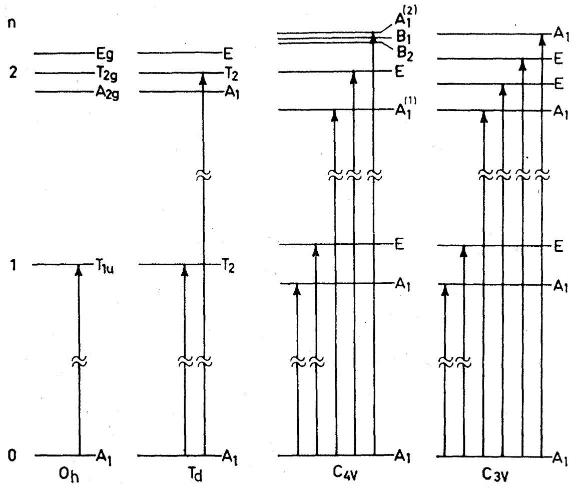

FIG. 4. Energy levels up to $n=2$ for a hydride ion situated in sites of $O_h$, $T_d$, $C_{4v}$, and $C_{3v}$ symmetry. Transitions observable by infrared absorption are indicated by vertical lines.

Application of unaxial stress[14] could lift the degeneracy of the line and provide a positive assignment of its site. Similarly, the observation of third-harmonic transitions could provide additional evidence. Both experiments are difficult due to the low intensity and large width of the fundamental transition.

The corresponding deuterium-ion transition has a frequency of 932 $\text{cm}^{-1}$ at room temperature. The ratio of hydrogen to deuterium frequencies is 1.39, and the deviation of this from the $\sqrt{2}$ represents the degree of approximation of the actual motion from an ideal localized mode for the hydride or deuteride ion.

### Axial Site

The two remaining lines in the spectra of rapidly quenched crystals are observed in all crystals containing RE ions. Their frequencies and linewidths are listed in Table I and are seen to vary with the particular RE ion present. Figure 5 shows typical absorption curves. The two lines always appear together and the high-frequency one is approximately twice as intense as the low-frequency one. The frequency separation of the lines is largest for lanthanum and decreases monotonically towards the end of the RE series. This is shown in Fig. 6.

In thick pieces of strongly hydrogenated crystals, second harmonics and combinations of the lines can be observed. These are listed in Table II for several RE ions, and the absorption curves are shown in Fig. 7. The lines can be assigned unequivocally only in crystals where the RE ion has no electronic absorption in the 2000-$\text{cm}^{-1}$ region. This restricts measurements to crystals containing lanthanum, gadolinium, RE ions in the latter part of the series, and yttrium. Owing to

---

[14] W. Hayes and H. MacDonald, Proc. Roy. Soc. (London) **A297**, 503 (1967).

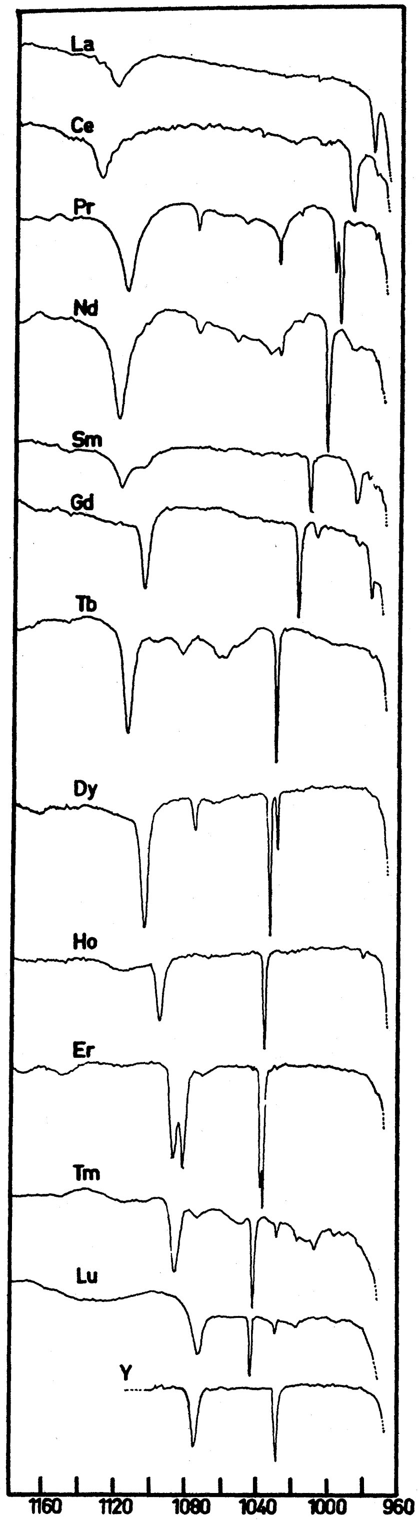

FIG. 5. Infrared absorption spectra of the axial-site hydride-ion centers in hydrogenated crystals of calcium fluoride containing RE recorded at 20°K. (Absorption due to yttrium contamination is observed in spectrograms of some of the RE ions.)

experimental limitations, it was not possible to measure the infrared absorption of crystals thicker than 30 mm, so no third harmonics were detected.

When the crystals are deuterated and rapidly quenched, lines appear which correspond to the absorption of the deuteride-ion axial site. For the crystals containing gadolinium the lines have frequencies and linewidths listed in Table III. The ratio of frequencies of corresponding hydride and deuteride ions is 1.381. It is more difficult to study the lines of the deuteride axial site since they fall in a region of strong absorption of the calcium-fluoride lattice.

### *Site Symmetry for the Hydride Ion*

Observation of a pair of absorption lines associated with the same hydride-ion site indicates an axial local symmetry. The number of second-harmonic absorption frequencies determines the type of axial symmetry of the site.

From the large variation of the frequencies of the lines with RE ions and from the occurrence of vibronic transitions (Sec. V), it is evident that the lines arise from hydride ions in close proximity to the RE ions. There are two possible axial sites for the hydride ion. One is for the hydride ion to replace a fluoride ion in the cube surrounding the RE ion, and the other is for the hydride ion to occupy an interstitial site in an adjacent empty cell and charge compensate the RE ion. The respective site symmetries are $C_{3v}$ and $C_{4v}$. Figure 4 shows the energy levels up to $n=2$ for $O_h$, $T_d$, $C_{3v}$, and $C_{4v}$ symmetries, with their group theoretical assignments and infrared activities. No second harmonic is allowed for the $O_h$ cubic symmetry, three second harmonics are expected for $C_{4v}$, and four for $C_{3v}$ symmetry. As only three second-harmonic transitions are observed in crystals containing gadolinium, thulium, or yttrium, the site can only have $C_{4v}$ symmetry since it is unlikely that one of the transitions remains accidentally degenerate for all three ions. This assignment is confirmed by ESR measurements on hydrogenated crystals containing cerium and neodymium (Sec. VII).

In the $C_{4v}$ site, the first excited vibrational state which is triply degenerate in the cubic symmetry is split into a doubly degenerate and a nondegenerate line, with intensity ratio 2:1. The doubly degenerate component is the higher-frequency member of the observed pair of lines and the nondegenerate component the lower.

### *Local Potential for the Hydride Ion*

The closeness of the hydrogen to deuterium frequency ratios to the square root of the two shows that one has a mode strongly localized around the light ions, and, to a good approximation, the neighboring ions may be considered static in this mode. The hydride ion then moves in a potential well which may be conveniently expanded in a power series in terms of the

TABLE I. Frequencies and linewidths in units of cm$^{-1}$ of infrared absorption lines observed in hydrogenated crystals of calcium fluoride containing RE ions.

| RE ion | Room temperature Frequency | Room temperature Linewidth | 77°K Frequency | 77°K Linewidth | 20°K Frequency | 20°K Linewidth |
|---|---|---|---|---|---|---|
| La | 1110 | | 976.6 | 1.8 | 976.9 | 1.0 |
| | | | 1121.0 | 9.8 | 1121.7 | 8.9 |
| Ce | 977 | 9.8 | 988.5 | 3.0 | 988.9 | 2.4 |
| | | | 1129.5 | 7.9 | 1130.1 | 6.6 |
| Pr | 986 | 9.2 | 994.7 | 2.6 | 994.7 | 1.2 |
| | 1106 | 25.7 | 1115.0 | 11.3 | 1115.0 | 8.8 |
| Nd | 990 | 10.2 | 1000.8 | 2.0 | 1001.5 | 1.4 |
| | 1101 | 22.7 | 1118.6 | 9.9 | 1119.4 | 6.8 |
| Sm | 1002 | 12.9 | 1011.4 | 1.7 | 1011.6 | 1.3 |
| | | | 1115.5 | 9.2 | 1117.3 | 7.4 |
| Gd | 1007 | 9.5 | 1016.8 | 1.8 | 1017.0 | 1.0 |
| | 1092.5 | | 1103.7 | 4.0 | 1104.2 | 3.5 |
| Tb | 1015 | 9.6 | 1028.9 | 1.5 | 1029.3 | 1.0 |
| | 1092 | 21.0 | 1112.3 | 4.7 | 1112.8 | 4.1 |
| Dy | 1019 | 10 | 1032.4 | 1.7 | 1033.1 | 1.0 |
| | 1088 | 15 | 1102.4 | 6.0 | 1103.3 | 3.0 |
| Ho | 1022 | 8 | 1034.8 | 2.0 | 1035.9 | 1.1 |
| | 1080 | 13 | 1903.0 | 5.8 | 1094.6 | 3.6 |
| Er[a] I | 1023 | 10.9 | 1035.8 | 1.6 | 1036.2 | 0.8 |
| | 1075 | 15.4 | 1085.6 | 5.2 | 1086.6 | 4.3 |
| Er[a] II | | | 1037.0 | | 1037.6 | 1.0 |
| | | | 1081.1 | 4.6 | 1081.2 | 3.5 |
| Tm | 1030 | 12.8 | 1043.1 | 1.4 | 1043.5 | 0.8 |
| | | | 1087.0 | 4.5 | 1087.3 | 4.1 |
| Lu | 1029 | 7.9 | 1042.1 | 1.2 | 1042.5 | 0.8 |
| | 1064 | 18.3 | 1072.0 | 6.5 | 1072.0 | 6.3 |
| Y | 1017.0 | 10.0 | 1028.6 | 1.3 | 1028.9 | 1.1 |
| | 1065 | 12.9 | 1074.3 | 4.0 | 1074.8 | 3.5 |

[a] Erbium is anomalous in having two sets of lines (see Fig. 5).

displacement. The terms appearing in the expansion depend on the symmetry of the site since the potential belongs to the totally symmetric representation of the site symmetry group. Expanding the potential appropriate to a $C_{4v}$-site symmetry to terms of the fourth degree yields

$$V=a(x^2+y^2)+bz^2+cz^3+dz(x^2+y^2)+f(x^4+y^4)+gz^4+hz^2(x^2+y^2)+kx^2y^2. \quad (1)$$

The vibrational energy levels of an ion of mass $m$ in this potential can be calculated by perturbation theory. The quadratic terms form a harmonic-oscillator potential, whose energy levels are

$$E(n_x,n_y,n_z)=\hbar(n_x+n_y+1)\omega_{\perp}+\hbar(n_z+\tfrac{1}{2})\omega_{\parallel}$$

where $\omega_{\perp}=(2a/m)^{1/2}$, and $\omega_{\parallel}=(2b/m)^{1/2}$, and $n_i$ is the occupation of the vibration mode in the $i$th direction. The ground state is nondegenerate, and there is a singlet (001) and a doubly degenerate [(100),(010)] first excited state. These energy levels are perturbed by the higher-order anharmonic terms, which allow ob-

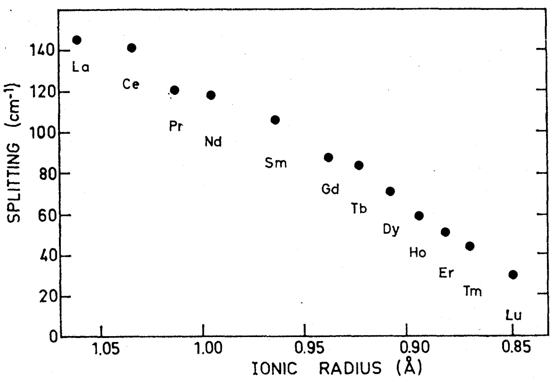

FIG. 6. Relation of the separation of the absorption lines of the axial-site hydrogen-ion center to the ionic radius of the adjacent rare earth.

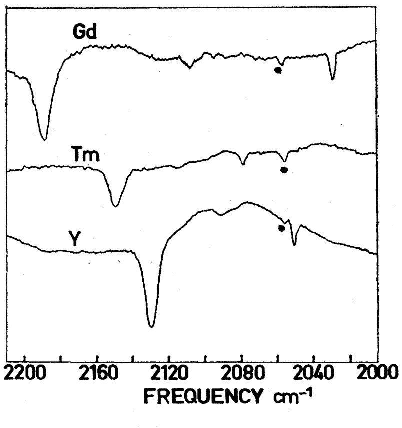

FIG. 7. Second-harmonic and combination lines observed in the absorption spectra of hydrogenated crystals of calcium fluoride containing gadolinium, thulium, or yttrium, recorded at 20°K. The line marked with an asterisk occurs in all three spectra and is not related to the axial site.

TABLE II. Frequencies and linewidths of harmonic and combination lines observed at 20°K in hydrogenated crystals of calcium fluoride containing RE ions. Units are $\mathrm{cm}^{-1}$.

| | Low-frequency second-harmonic line | | | Combination line | | | High-frequency second-harmonic line | | |
|---|---|---|---|---|---|---|---|---|---|
| RE | Frequency | Linewidth | Anharmonic shift | Frequency | Linewidth | Anharmonic shift | Frequency | Linewidth | Anharmonic shift |
| Gd | 2029.2 | 3.3 | −4.8 | 2108.5 | 5.3 | −14.7 | 2189 | 7.5 | −19.4 |
| Tm | 2080.0 | 3.4 | −7.0 | 2115.5 | 4.5 | −15.3 | 2150.5 | 9.2 | −24.1 |
| Y | 2051.7 | 2.5 | −6.0 | 2094 | 6.0 | − 9.7 | 2130.2 | 7.5 | −19.4 |

servation of harmonics of the main transition. The quartic terms contribute to the diagonal elements and the cubic terms to the off-diagonal elements of the energy matrix. Table IV gives the resultant energy scheme to the first order in perturbation theory.

Six unknown constants $a$, $b$, $f$, $g$, $h$, and $k$ are needed to determine the energy levels of the first- and second-harmonic transitions. There are only five transitions to these levels observable by infrared absorption, so the problem is overspecified.

Nevertheless, one can use the observed absorption frequencies of the gadolinium-doped crystal (Tables I and II) and solve for unknowns $a$, $b$, $g$, $h$, and $3f+\frac{1}{2}k$. The results are

$$a=(3.80\pm0.04)\times10^4 \text{ erg cm}^{-2},$$

$$b=(3.18\pm0.03)\times10^4 \text{ erg cm}^{-2},$$

$$h=-(26.3\pm8)\times10^{19} \text{ erg cm}^{-4},$$

$$g=-(3.03\pm0.9)\times10^{19} \text{ erg cm}^{-4},$$

and

$$3f+\tfrac{1}{2}k=-(43.6\pm6)\times10^{19} \text{ erg cm}^{-4}.$$

The corresponding frequencies $\nu_x$ and $\nu_y$, in the harmonic approximation, are $\nu_y=\nu_x=1130\pm4.5$ $\mathrm{cm}^{-1}$ and $\nu_z=1034.5\pm6.5$ $\mathrm{cm}^{-1}$. The negative sign of $h$, $g$, and $3f+\frac{1}{2}k$ is physically significant, as shown in the next section.

An estimate of the degree of anharmonicity can be deduced from the frequency shift of observed second-harmonic lines away from twice the fundamental frequencies. These data are shown in Table II. The deviations observed are comparable to the anharmonic shifts of the 965-$\mathrm{cm}^{-1}$ line in pure calcium fluoride[1] and hydride-ion localized modes in the lanthanum trifluorides.[15]

TABLE III. Axial-site frequencies and linewidths in units of $\mathrm{cm}^{-1}$ of the infrared absorption lines observed in deuterated crystals of calcium fluoride containing gadolinium.

| Room temperature | | 77°K | | 20°K | |
|---|---|---|---|---|---|
| Frequency | Linewidth | Frequency | Linewidth | Frequency | Linewidth |
| 728 | ~10 | 735.5 | ~3 | 735.5 | 3 |
| 792 | 8 | 799.2 | 3.1 | 799.7 | 3.2 |

### *Interaction between Adjacent RE and Hydride Ions*

The frequency separation between the two infrared transitions of the $C_{4v}$ axial site is a measure of the perturbing effect of a RE ion on the triply degenerate transition of an interstitial cubic site. The increased attraction of an extra charge on the RE ion shifts the equilibrium positions of the two ions closer to one another than are the centers of their respective cubes (Fig. 8).

Let us assume that the hydride ion moves in a field which is a combination of the undeformed cubic potential of an isolated interstitial site and the electrostatic attraction of an extra positive charge in the adjacent cube. The equilibrium position is the minimum of the new compound potential.

Expansion of the cubic potential to the fourth term in the displacement coordinates around the center of the cube yields

$$\begin{aligned}V=A(x^2+y^2+z^2)+B(x^4+y^4+z^4)\\+C(x^2y^2+x^2z^2+y^2z^2)\\-\sigma e^2[(a^*-z)^2+x^2+y^2]^{-1/2}.\end{aligned}\quad(2)$$

Here $a^*$ represents the separation between the center of the hydride cube and the shifted equilibrium position of the RE ion, and $\sigma$ represents a constant determining the effective screened attraction.

The coefficients in (1) and (2) are interrelated, and a comparison can be made if the potential (2) is expanded around its equilibrium position $(0,0,z_0)$.

The coefficients of the even terms in the two expressions satisfy

$$a=A+Cz_0^2+\tfrac{1}{2}\sigma e^2(a^*-z_0)^{-3},\quad(3)$$

$$b=A+6Bz_0^2-\sigma e^2(a^*-z_0)^{-3},\quad(4)$$

$$f=B-\tfrac{3}{8}\sigma e^2(a^*-z_0)^{-5},\quad(5)$$

$$g=B-\sigma e^2(a^*-z_0)^{-5},\quad(6)$$

$$h=C+3\sigma e^2(a^*-z_0)^{-5},\quad(7)$$

$$k=C-\tfrac{3}{4}\sigma e^2(a^*-z_0)^{-5}.\quad(8)$$

The observed frequencies for the cubic and axial sites are approximately given by their harmonic values $\omega_c=(2A/m)^{1/2}$, $\omega_\perp=(2a/m)^{1/2}$, $\omega_{\parallel}=(2b/m)^{1/2}$. Using these values, the values for gadolinium-doped $\mathrm{CaF}_2$, $g$,

---

[15] G. D. Jones and R. A. Satten, Phys. Rev. **147**, 566 (1966).

TABLE IV. Zero- and first-order energy, representations, wave functions, and infrared (IR) activity of the anharmonic oscillator in tetragonal symmetry potential.[a]

| $n$ | Zero-order energy | Representation | Eigenvectors | First-order energy correction | IR activity |
|---|---|---|---|---|---|
| 0 | 0 | $A_1$ | $\|000\rangle$ | $(3/4\beta^2)g+(3/2\alpha^2)f+(1/2\alpha\beta)h+(1/4\alpha^2)k$ | $z$ |
| 1 | $\hbar\omega_z$ | $A_1$ | $\|001\rangle$ | $(15/4\beta^2)g+(3/2\alpha^2)f+(3/2\alpha\beta)h+(1/4\alpha^2)k$ | $z$ |
|  | $\hbar\omega_x$ | $E$ | $\|100\rangle$<br>$\|010\rangle$ | $(3/4\beta^2)g+(9/2\alpha^2)f+(1/\alpha\beta)h+(3/4\alpha^2)k$ | $x,y$ |
| 2 | $2\hbar\omega_z$ | $A_1^{(1)}$ | $\|002\rangle$ | $(39/4\beta^2)g+(3/2\alpha^2)f+(5/2\alpha\beta)h+(1/4\alpha^2)k$ | $z$ |
|  | $\hbar(\omega_x+\omega_z)$ | $E$ | $\|101\rangle$<br>$\|011\rangle$ | $(15/4\beta^2)g+(9/2\alpha^2)f+(3/\alpha\beta)h+(3/4\alpha^2)k$ | $x,y$ |
|  | $2\hbar\omega_x$ | $B_2$ | $\|200\rangle-\|020\rangle$ | $(3/4\beta^2)g+(21/2\alpha^2)f+(3/2\alpha\beta)h+(3/4\alpha^2)k$ | ... |
|  |  | $A_1^{(2)}$ | $\|200\rangle+\|020\rangle$ | $(3/4\beta^2)+g(21/2\alpha^2)f+(3/2\alpha\beta)h+(7/4\alpha^2)k$ | $z$ |
|  |  | $B_1$ | $\|110\rangle$ | $(3/4\beta^2)g+(15/2\alpha^2)f+(3/2\alpha\beta)h+(9/4\alpha^2)k$ | ... |

[a] The energy parameters are given in Eq. (1), Sec. IV B; $\alpha=M\omega_x/h=M\omega_y/h$, $\beta M\omega_z/h$.

$h$, and $3f+\frac{1}{2}k$ given in the previous section, and the equilibrium equation

$$Az_0+2Bz_0^3-\tfrac{1}{2}\sigma e^2(a^*-z_0)^{-2}=0, \tag{9}$$

yield a set of six independent equations for the five unknowns $B$, $C$, $\sigma$, $a^*$, and $z_0$. The problem is overdetermined, and an attempt to solve the equations shows that they are incompatible. This indicates that the electrostatic model and approximations leading to Eqs. (3)–(9) are crude and are not reliable for numerical estimates. Nevertheless, if we assume that $\sigma=1$ in Eqs. (5) and (9), then $z_0=0.5$ Å as an upper limit. One can then substitute the values derived from Eqs. (6) and (7) for $B$ and $C$ in Eqs. (3) and (4). It follows that $\omega_\perp$, the frequency of the transverse vibration, is higher than $\omega_\parallel$ the longitudinal frequency, for values of $\sigma$ larger than 0.18.

The inadequacy of the electrostatic model and the fact that the cubic frequency $\omega_c=1300$ cm$^{-1}$ does not fall between the two axial-site frequencies when $B=C=0$ can be explained as follows: The apparent negative charge on the hydride ion varies with the physical environment of the ion. Since the electron affinity of a neutral hydrogen atom is small, the hydride ion readily shares its electron with a trivalent RE ion and forms a covalent bond. The hydride ion thus finds itself with a reduced effective charge. A neutral hydrogen atom has a frequency of 767 cm$^{-1}$ in the axial site (Sec. VI). The hydride ion has a mean frequency of 1070 cm$^{-1}$, and the cubic site has frequency 1300 cm$^{-1}$. In each case, the potential acting on the hydride ion consists of electrostatic and nonelectrostatic parts. If we assume that the cubic-site hydride ion has full electronic charge, and the neutral hydrogen atom site has zero charge, then the effective charge on the hydride ion in the axial site has some intermediate value, and its mean frequency should fall between the frequency of the cubic site and that of the neutral hydrogen axial site.

The mean frequency of the axial-site hydride lines is almost constant along the RE series, indicating virtually identical charge transfer for all the ions.

### Separation of the Lines

The frequency separation of the axial-site lines decreases monotonically along the RE series and can be correlated with variation of the ionic radius of the ions. Yttrium, although not a member of the RE series, obeys the same separation versus ionic radius relation-

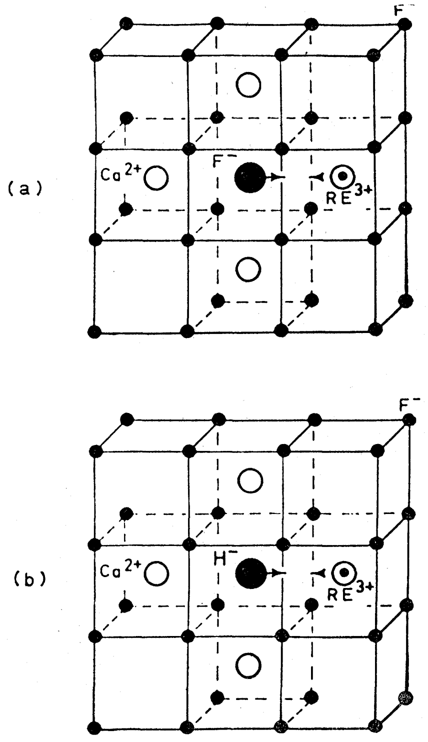

FIG. 8. Schematic representation of (a) the fluoride- and (b) the hydride-ion charge-compensation sites.

ship. Its ionic radius is 0.88 Å.[16] It should be noted in Fig. 5 that the absorption lines associated with yttrium appear as traces in crystals doped with each of the RE ions. This is due to the insufficient purity of our raw materials.

Consideration of Eqs. (3) and (4) and the equilibrium condition Eq. (9) shows that the frequency separation depends strongly on the electrostatic attraction between the two ions. This attraction varies with the magnitude of $\sigma$ and the related equilibrium shift $z_0$.

For ions of large radius, at the beginning of the RE series, the four $F^-$ ions which lie in the plane separating RE and the $H^-$ ions are pushed sideways. This decreases the screening and increases the electrostatic attraction and explains the large separation of the axial lines for La, Ce, and their neighbors (Table I, Fig. 5). As one moves to the end of the series, the ionic radius decreases, and the fluorines approach one another screening and reducing the electrostatic attraction. The frequency separation is correspondingly reduced. Note also that the ionic radius of $Ca^{2+}$ is approximately in the middle of the range of RE radii.

This explanation is consistent with the greater stability of tetragonal charge compensation which one finds in ions at the begining of the RE series. Tetragonal compensation in nonhydrogenated $CaF_2$ is due to an interstitial $F^-$ ion. It is much more common and stable at the beginning of the RE series than at the end.[2] The axial site is very stable and strong in hydrogenated crystals also at the expense of a weak cubic site at the beginning of the series. The reverse situation of a strong cubic site and a weak axial site is characteristic of ions at the end of the series.

### *Linewidths*

The widths of the two lines differ. The width of the lower-frequency nondegenerate line is very similar to width of the 965-$cm^{-1}$ line of the hydride ion substituted in pure calcium fluoride.[1] It has a residual width of 1 $cm^{-1}$ in all the rare earth crystals at 20°K and broadens with increase in temperature to become 10 $cm^{-1}$ at room temperature. The upper-frequency doubly degenerate line has a larger residual linewidth at low temperatures which varies along the RE series and is greatest near the ends where the RE ions are of different ionic size than the substituted calcium ion. The following broadening mechanisms may be responsible for the linewidths:

(1) The lifetime of the transverse-mode first-excited vibrational level due to tunneling of the hydride ion from its interstitial position to equivalent adjacent sites may be responsible for the linewidths.[17]

The wave function of the first excited state of this mode has a node at the equilibrium point and consequently extends into the potential barrier between equivalent interstitial sites. The ground-state wave function or that of the first excited level of the longitudinal vibration has a much smaller extension in the corresponding direction with a much-reduced tunneling rate. Thus, lifetime broadening due to this effect is expected to be much more pronounced for the transverse vibration than for the longitudinal vibration. We observed this effect in the infrared absorption as well as in the vibronic emission of gadolinium.

The tunneling rate does not strongly depend on the temperature and indeed the width of the transverse line changes moderately with temperature (Table I).

The tunneling rate decreases when the mass of the moving particle increases. One thus expects a narrower linewidth due to transverse vibration in deuterated crystals than in hydrogenated crystals. Such variation is difficult to observe by infrared absorption since the deuterium lines are partly swamped by strong absorption in the host lattice. However, deuterated crystals have a narrower linewidth of vibronic transitions than hydrogenated crystals and this strikingly confirms the expected variation of linewidth with mass.

(2) A transition from the higher- to the lower-frequency energy level of the two excited states can occur, accompanied by the spontaneous emission of lattice phonons of frequency equal to the energy-level separation, and cause broadening of levels. At low temperatures, only the upper level is affected, but at high temperatures the lower level is also broadened with respect to the upper level in the ratio $e^{-h\nu/kT}$. This direct transition broadening involves the third or higher power of the frequency separation $\nu$ of the levels. (Relaxation rate involving optical phonons depends on the third power and that due to acoustical phonon on the fifth power of the frequency separation of the levels.[18]) and so is more conspicuous for the first part of the RE series. The infrared data does not reveal such simple and marked regularity and thus at low temperature this mechanism must yield a small contribution to the observed broadening.

Erbium is anomalous in having two sets of lines. Possibly some erbium ions are located in other sites slightly perturbed from the usual ones.

(3) Random variations in the exact configuration of ions around the hydride ion can also cause incipient splitting of the doubly degenerate levels giving rise to a larger over-all width. Such random variations could be more prominent in those cases where the RE ion is of markedly different size from the substituted calcium ion. It seems unlikely, though, that the observed splitting is random in all trivalent ions and a uniform distortion would cause splitting rather than broadening. This was never observed.

---

[16] T. Moeller, *The Chemistry of the Lanthanides* (Reinhold Publishing Corp., New York, 1963).

[17] W. Vedder and D. F. Hornig, in *Advances in Spectroscopy*, edited by H. W. Thompson (John Wiley & Sons, Inc., New York, 1962), Vol. II.

[18] R. Orbach, Proc. Roy. Soc. (London) **265**, 1 (1962).

TABLE V. Frequencies and assignment of the emission lines of the transition ${}^6P_{7/2} \rightarrow {}^8S_{7/2}$ observed at 77 and 195°K in hydrogenated and deuterated crystals of calcium fluoride which contain 0.05% gadolinium and which were rapidly quenched following hydrogenation.

| Site label | Assignment | 77°K Wavelength (Å) | 77°K Frequency ($cm^{-1}$) | 195°K Wavelength (Å) | 195°K Frequency ($cm^{-1}$) |
|---|---|---|---|---|---|
| *A* | fluoride ion charge-compensated site | 3120.85 | 32033.3 | 3120.44 | 32037.5 |
| | | 3113.50 | 32108.9 | 3113.36 | 32110.3 |
| | | 3109.67 | 32148.4 | 3109.64 | 32148.8 |
| | | 3108.46 | 32161.0 | 3108.51 | 32160.5 |
| *C* | cubic gadolinium site | 3120.64 | 32035.5 | . . .[a] | . . . |
| | | 3119.14 | 32050.9 | 3118.86 | 32053.7 |
| | | 3115.08 | 32092.6 | 3114.94 | 32094.1 |
| *T* | trigonal oxygen site | 3146.73[b] | 31769.8 | 3146.40[c] | 31773.2 |
| | | 3135.69 | 31881.7 | 3135.50 | 31883.6 |
| $H^-$ | tetragonal hydride ion site | 3131.22 | 31927.2 | 3130.61 | 31933.3 |
| | | 3120.90 | 32033.0 | 3120.95[d] | 32032.3 |
| | | 3114.58 | 32097.8 | | |
| | | 3110.52 | 32139.7 | | |
| $D^-$ | tetragonal deuteride ion site | 3131.42 | 31925 | 3130.76 | 31931.8 |
| | | . . .[e] | . . . | 3121.00 | 32031.8 |
| | | 3114.60 | 32097.6 | 3114.43 | 32099.3 |
| | | 3110.50 | 32139.9 | 3110.56 | 32139.3 |
| $H^0$ | tetragonal hydrogen atom site | 3126.01 | 31980.4 | | |
| | | 3117.37 | 32069.1 | | |
| | | 3113.02 | 32113.9 | | |
| | | 3110.52 | 32139.7 | | |
| $D^0$ | tetragonal deuterium atom site | 3125.94 | 31981.2 | | |
| | | 3117.37 | 32069.1 | | |
| | | 3113.01 | 32114.0 | | |
| | | 3110.50 | 32139.9 | | |
| . . . | unassigned line present in unhydrogenated crystal | 3122.96 | 32011.6 | | |
| . . . | unassigned line appearing after hydrogenation, but not related to either the *H* or $H^0$ site | 3116.00 | 32083.3 | | |

[a] This line is hidden under the first strong line of the *A* site.
[b] The other two lines of this site were not observed in this work.
[c] The other two lines of this site were not observed in this work.
[d] This line's frequency is only approximate due to proximity of the first strong line of the *A* site.
[e] This line hidden under the first strong line of the *A* site.

At liquid-air temperature or lower, the observed widths can be explained strictly due to tunneling. At higher temperatures, relaxation contributes increasingly, and both processes are responsible for the observed width.

## V. ELECTRONIC AND VIBRONIC SPECTRA

When a hydride ion occupies a site near a RE ion, the energy levels of the latter are perturbed by the change in the environment, and new spectral lines appear [Fig. 9(a)]. These lines can be removed by heating the crystals in vacuum at 900°C for several hours to remove the hydrogen. Since, in general, the number of RE ions and their valency do not change during the hydrogenation process, the new hydrogenic sites grow at the expense of existing sites. In particular, we observed such growth at the expense of the $F^-$-compensated tetragonal site (Site A, Table V). Of the RE ions, gadolinium is particularly well suited for studying such site transformations. Its spectrum is simple, and the main transitions appear strongly in fluorescence. Furthermore, the various sites of the non-

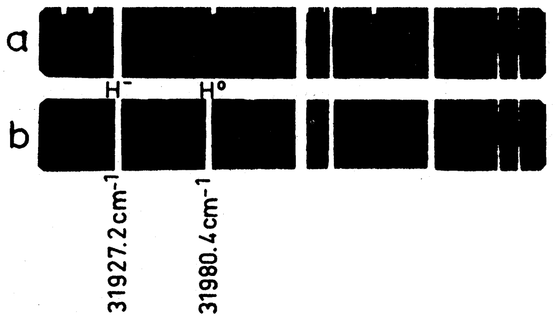

FIG. 9. Emission spectra of gadolinium in hydrogenated $CaF_2$ before (a), and after (b), uv irradiation.

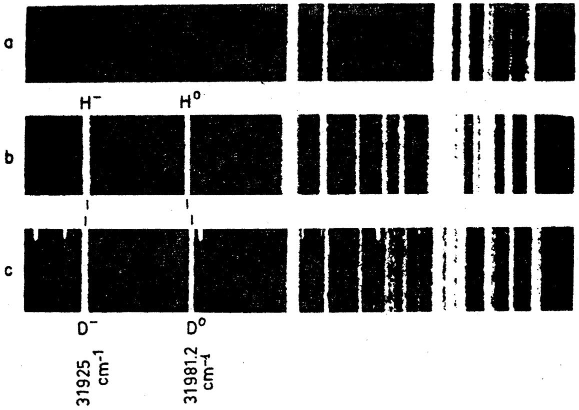

FIG. 10. uv emission of calcium fluoride containing gadolinium compared with that from the same crystals following hydrogenation or deuteration, and subsequent uv irradiation. Two hydrogenic sites ($H$ and $H^0$) and two deuterium sites ($D$ and $D^0$) are created; the lines show an isotope shift different for the two centers.

hydrogenated crystals containing gadolinium have been extensively investigated by Makovsky. In the present paper the following notation of Makovsky[19] is used for the different gadolinium sites in $CaF_2$: The $F^-$ compensated tetragonal site is denoted by $A$, the cubic site by $C$, the $O^{2-}$ compensated trigonal site by $T$, and $H^-$, $D^-$ and $H^0$, and $D^0$ are tetragonal sites in which $H^-$, $D^-$, $H^0$, or $D^0$ are interstitially located at the center of an empty cube adjacent to the gadolinium.

A strong emission in the transition ${}^6P_{7/2} \rightarrow {}^8S_{7/2}$ of gadolinium was observed in hydrogenated crystals of calcium fluoride. It is found that hydrogenation produces many new lines in the fluorescence spectrum indicative of the formation of a multitude of new hydrogenic sites.[13]

For rapidly quenched crystals not subjected to uv radiation, only one new hydrogenic site is formed. This is labelled as the $H^-$ site in Table V. Figure 9(a) shows some spectragrams of the uv emission lines of $Gd^{3+}$ in the hydrogenic site. A comparison with the spectra of the unhydrogenated crystal is given in Fig. 10.

TABLE VI. Frequencies and assignment of the local-mode vibronics observed in hydrogenated and deuterated crystals of calcium fluoride containing 0.05% gadolinium, recorded at 77°K.

| Impurity | Vibronic frequency (cm⁻¹) | Parent electronic frequency (cm⁻¹) | Separation (cm⁻¹) | Corresponding infrared absorption frequency (cm⁻¹) |
|---|---|---|---|---|
| $H^-$ | 30910 | 31927.2 | 1017 | 1016.8 |
| | 30823 | 31927.2 | 1104 | 1103.7 |
| $D^-$ | 31189 | 31925 | 736 | 735.5 |
| | 31127 | 31925 | 798 | 799.2 |

In Table V we have listed the electronic lines of the various sites in the crystals both before and after hydrogenation, and at a temperature of 77°K. In Table V the same is given for 195°K.

The deuterated crystals in these tables exhibit gadolinium $D^-$-site lines which are slightly shifted relative to those of the hydrogenic site (Fig. 10). Such isotope shifts have previously been reported for praseodymium and neodymium fluorides.[15] The isotope shift proves that the new gadolinium sites are associated with hydrogen or deuterium. The electronic transitions of the hydrogenic sites exhibit weak vibronic emission lines on their long-wavelength side (Fig. 11).

Each Stark component of the emitting electronic multiplets gives rise to two vibronic lines associated with the two frequencies of the axial mode. Tables VI and VII list the vibronic emissions at 77 and 195°K, respectively. Intensities of the vibronic lines are proportional to the populations of emitting Stark components. Owing to the fast relaxation within the Stark multiplet, these populations obey a Boltzmann distribution at ambient temperatures. Hence, lines associated with the upper components of the multiplet can be observed only at higher temperatures.

Vibronic transitions of the longitudinal mode in the axial site are much stronger than the vibronics of the transverse mode. This is plausible since the longitudinal mode has a stronger interaction with the RE ion.

### Site Symmetry and Crystal Field for the Gadolinium Ion

The close correspondence of the vibronic frequency intervals to the axial-site infrared-absorption frequencies of the hydride ion shows that the new hydrogenic site of the gadolinium ion is indeed associated with the axial site of the hydride ion. The environment of the gadolinium ion is, therefore, as shown in Fig. 8(b), and the gadolinium has site symmetry $C_{4v}$. This site (labelled $H^-$ in Table V) is, thus, the hydrogen analog of the well-characterized fluoride-ion charge-compensated tetragonal site ($A$ site) found in the parent crystals, as shown in Fig. 8(a). The Stark splitting patterns for the two sites are very similar (Fig. 12).

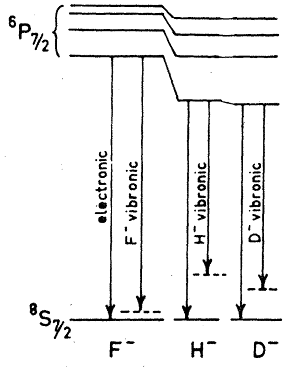

FIG. 11. Energy-level scheme for the electronic- and local-mode vibronic lines observed in fluorescence as the ${}^6P_{7/2}$-${}^8S_{7/2}$ transition in calcium-fluoride crystals containing gadolinium.

---

[19] J. Makovsky, in *Proceedings of the Physics Quantum Electronics Conference*, edited by P. L. Kelley, B. Lax, and P. E. Tannenwald (McGraw-Hill Book Co., New York, 1966), p. 340; Phys. Letters **19**, 647 (1966).

A new site related to these is the hydrogen-atom site obtained by uv irradiation of hydrogenated crystals. The Stark splitting pattern of the site (labelled $H^0$ in Table V) is also shown in Fig. 12.

The splitting pattern for the ${}^6P_{7/2}$ $A$-site multiplet of gadolinium in calcium fluoride has been discussed by Nerenberg and Schlesinger.[20] A similar analysis is applicable to the hydrogenic sites. The splitting of the ${}^6P_{7/2}$ multiplet in the tetragonal crystal field is given by the expression

$$\frac{\langle {}^6P_{7/2}|H_{\mathrm{so}}|{}^6D_{7/2}\rangle\langle {}^6D_{7/2}|A_0{}^2V_0{}^{(2)}|{}^6P_{7/2}\rangle}{E_{{}^6P_{7/2}}-E_{{}^6D_{7/2}}},$$

where $H_{\mathrm{so}}$ represents the spin-orbit interaction and $A_0{}^2V_0{}^{(2)}$ represents the crystal-field terms involving spherical harmonics of second degree.

The spin-orbit matrix elements are almost identical for all three tetragonal sites ($H^-$, $H^0$, and $A$), and the magnitude of the splitting is determined by the crystal field matrix element. In this approximation, the splitting patterns of the three tetragonal sites should be related to one another by a simple scale factor. Figure 12 shows that the observed patterns do approximate this behavior.

### Isotope Shift

Deuterated crystals of calcium fluoride containing gadolinium show sites whose frequencies differ slightly from those produced by hydrogenation. This isotope shift can be derived from the frequencies listed in Tables V and VI and is of the order of 1 cm$^{-1}$. It is comparable to the shifts observed in hydrogenated crystals of praseodymium and neodymium fluorides.[15] Figure 10 shows the isotope shift as observed for the lowest-frequency emission lines of both the $H^-$ and the $H^0$ sites.

The isotope shift arises through a coupling of the local-mode vibrations of hydrogen and deuterium to the electronic states of the gadolinium ion. The widely different zero-point amplitudes of vibration for hydrogen and deuterium ions result in different perturbations of the gadolinium ion's electronic states. The appearance of the isotope shift depends on the electron-phonon interaction $V_{\mathrm{ev}}$, in which the crystal field at the gadolinium $4f$ electrons is modulated by the vibrational motion. The interaction has the form

$$V_{\mathrm{ev}}=\sum_i f_i{}^aQ_i{}^a+\sum_{ij} g_{ij}{}^{ab}Q_i{}^aQ_j{}^b.$$

The $Q$'s represent normal coordinates of the lattice and $f$ and $g$ functions of the electronic coordinates of the $4f$ electrons. Previous calculations[15] in praseodymium and neodymium fluorides indicate that the main contribution to the isotope shift comes from the second-degree term in a first-order perturbation. The level shift of hydrogen relative to deuterium can turn out to be either positive or negative, depending on the sign of the expectation value $\langle g\rangle$ of the electronic contribution to the electron-phonon interaction.

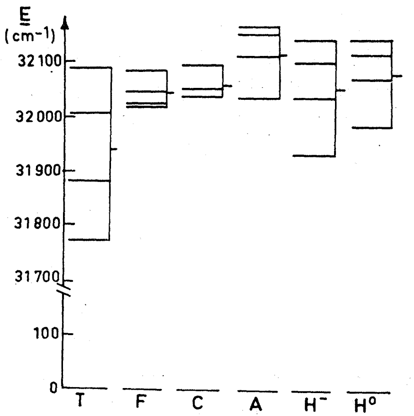

FIG. 12. Energy-level schemes and centers of gravity for the ${}^6P_{7/2}$ multiplet in different Gd$^{3+}$ sites in CaF$_2$. (Site designation follows Ref. 19.)

The observed isotope line shift is the difference between the level shift of the ground ${}^8S_{7/2}$ and that of the excited ${}^6P_{7/2}$ states. To calculate the isotope shift for a given electronic level requires a knowledge of the electronic wave functions of the gadolinium ion for the level in a tetragonal crystalline field. Gadolinium has a half-filled shell, so all crystal-field matrix elements within a given $L$ multiplet vanish, and it is necessary to consider crystal-field admixture of other $L$ multiplets

TABLE VII. Frequencies and assignment of the local-mode vibronics as observed in hydrogenated calcium fluoride containing 0.05% gadolinium at 195°K.

| Ion | Vibronic frequency (cm$^{-1}$) | Parent electronic frequency (cm$^{-1}$) | Separation (cm$^{-1}$) |
|---|---|---|---|
| $H^-$ | 30920 | 31933.3 | 1013 |
| | 30834 | 31933.3 | 1099 |
| | 31018 | 32032.3[a] | 1014 |
| | ...[b] | 32032.3[a] | ... |
| | 31086 | 32099.4 | 1013 |
| | 31000 | 32099.4 | 1099 |
| | 31125.5 | 32139.0 | 1013.5 |
| | 31040.5 | 32139.0 | 1098.5 |
| $D^-$ | 31199 | 31931.8 | 733 |
| | 31135 | 31931.8 | 797 |
| | ... | ... | ... |
| | 31237 | ~32032 | ~795 |
| | 31367 | 32099.3 | 733 |
| | ~31302 | 32099.3 | ~798 |
| | ... | ... | ... |
| | 31342 | 32139.3 | ~797 |

[a] This line's frequency is only approximate as the line is very close to the strong $A_1$ line of the tetragonal $A$ site.

[b] This line was not observed as it is obscured by the nearby 30920-cm$^{-1}$ vibronic.

---

[20] M. Nerenberg and M. Schlesinger, Phys. Letters **26A**, 109 (1968).

through the spin-orbit interaction to account for the observed energy-level scheme. This, together with the uncertainties in the relevant crystal-field parameters and wave functions for the $^8S_{7/2}$ ground state, make it impracticable to attempt detailed calculations of the observed isotope shifts.

The sensitivity of the observed isotope shift to the exact nature of the electronic wave functions of the gadolinium ion is shown by the reversal in isotope shift shown by corresponding lines of the $H^-$ and $H^0$ sites (Fig. 10).

### Lifetimes of the $^6P_{7/2}$ Electronic States

Preliminary lifetime measurements have been made on the various fluorescence transitions. At 77°K the $A$ site has a fluorescence lifetime of $11\pm1$ msec, the $H^-$ site $4\pm0.5$ msec, the $D^-$ site 3 msec, and the $H^0$ and $D^0$ sites $8\pm1$ msec. The trigonal site $T$ obtained in oxygenated crystals shows a lifetime of $1.5\pm0.5$ msec. The similarity of the lifetimes for the hydrogenic and corresponding deuterium sites shows that multiphonon relaxation mechanism involving the localized phonons do not play a major role in determining the lifetimes of the upper electronic states at 77°K.

The dominant mechanism determining the lifetime of the $^6P_{7/2}$ levels at 77°K is the radiative transition probability due to spontaneous emission. A general discussion of radiative transition probability of RE ions in crystals is found in Ref. 21.

For the comparisons between lifetimes of the different sites, it is sufficient to consider the general behavior of the electric dipole matrix elements between the mixed parity states without going into the precise details of the interactions. The three sites $A$, $H^0$, and $H^-$ have similar patterns whose crystal-field splittings are in the ratio 1:1.25:1.67. With the assumption of exact proportionality of all (odd and even) $A_1{}^m$ components of the crystal field, the line strength $S$ of the corresponding transitions in all three sites will be in the ratio of the squares of the corresponding crystal-field parameters. The transition probabilities will, therefore, be in the ratios 1:1.56:2.78 and the lifetimes of the fluorescent transitions in the inverse ratios. If the measured lifetime of 11 msec for the $A$ site is taken as due to spontaneous emission only, the corresponding values for the $H^0$ and $H^-$ sites should be 7 and 4 msec, respectively. These values fall close to those actually observed. This shows that the emission lifetimes at 77°K are mainly determined by radiative processes, through forced electric dipole transitions. The contribution of magnetic dipole transitions to the emission probability is negligibly small since the inherently weak probability of magnetic transitions is further reduced by the different multiplicities of the two states.

### Temperature Dependence of the Fluorence Lines

Temperature-dependence studies on the fluorescence lines of the hydrogenic gadolinium site has revealed the following striking phenomenon: The electronic lines and their associate vibronics decrease very rapidly in intensity at 220°K and are completely absent at room temperature. The temperature of steepest decrease for the deuterated crystals is approximately 10° higher than for the hydrogenated crystals. The decrease in intensity occurs over the temperature range of 30–60°K in the hydrogenated and deuterated crystals, respectively. The infrared absorption lines of the axial site do not reveal any abrupt intensity changes at the transition temperature of the electronic emission.

There are indications that new electronic lines associated with a new hydrogenic site of a different symmetry appear above the transition temperature. The axial atomic $H^0$ site shows a similar disappearance of electronic emission at a transition temperature of about 100°K.

We believe that the disappearance of the electronic line may be due to a very fast tunneling of the $H^-$ ion between six equivalent surrounding interstitial sites. Above the transition temperature, the central gadolinium sees an "effective" cubic potential with the $H^-$-ion charge smeared evenly into the six adjacent cubes. Further work is needed to elucidate this point and the results will be reported elsewhere.

## VI. IRRADIATION AND THE THERMAL EFFECTS

We have irradiated the hydrogenated crystals of calcium fluoride which contain gadolinium at liquid-nitrogen temperature, and when the uv radiation is shorter than 2500 Å, the electronic lines of the axial site decrease in intensity and a new site, designated $H^0$ in Table V, appears [Fig. 9(b)].

The existence of an isotope shift for this new site shows that it is associated with hydrogen. Vibronic transitions are also observed which are separated from their parent lines by 767 and 565 cm$^{-1}$ for hydrogenated and deuterated crystals, respectively (Table VIII).

The ratio of the hydrogen to deuterium local-mode frequency is 1.36 (compare $H^-$ axial mode ratio 1.38).

The low vibration frequencies indicate interaction force constants of the $H^0$ atoms with their neighbors that are much reduced compared with the constants for $H^-$ ions.

Attempts were made to detect these vibrations by direct infrared absorption, but met with no success at the spectrometer sensitivity used. This negative result sets an upper limit for the oscillator strength of these modes as compared with the hydride localized ion modes at 1017 and 1104 cm$^{-1}$. If the linewidth is assumed to be 2 cm$^{-1}$, this upper limit is 1/100 and is proportionally larger for broader lines.

To explain these results, it is postulated that the uv radiation converts the hydride ion into a neutral

---

[21] B. G. Wybourne, in *Spectroscopic Properties of Rare Earths* (John Wiley & Sons, Inc., New York, 1965).

hydrogen atom. Because the irradiation is at low temperature, we expect no transfer of atoms to different sites, and the new site consists of a gadolinium ion and a neutral hydrogen atom $H^0$ in adjacent interstitial sites. The association of the new site with the formation of a neutral hydrogen atom *in situ* is supported by the following argument: Bessent *et al.*[22] have shown that x irradiation of hydrogenated $CaF_2$ at sufficiently low temperatures ionizes the hydride ions and leaves neutral atoms at their previous lattice sites. In our case also, the new $H^0$ site can be generated by x irradiation of the $CaF_2$: Gd hydrogenated crystal at 77°K.

The resulting assignment of $C_{4v}$ site symmetry is also supported by the strong similarity between the $H^0$ Stark pattern and the $H^-$ and $F^-$ tetragonal spectra. The motion of hydrogen atom is not associated with infrared absorption, yet the vibration of the neutral atom modulates the ion-pair interaction to give a vibronic spectrum.

Weak infrared absorption is expected for the neutral $H^0$ motion due to the Lax-Burnstein mechanism.[23] The absence of such absorption in our case shows that this effect is small for the hydrogen atom is $CaF_2$.

The data in Table IX shows that only one local-mode frequency (767 $cm^{-1}$ in $H^0$ and 565 $cm^{-1}$ in $D^0$) appears as a vibronic frequency separation. The relatively low frequency indicates that the hydrogen atom is less tightly bound to the lattice than the hydride ion. The vibration frequency of a neutral hydrogen atom in ionic lattice was first demonstrated by the ESR relaxation time measurement of Feldman and coworkers.[24] A value of $590.5\pm41.7$ $cm^{-1}$ was estimated for the vibration frequency of $H^0$ atoms in $CaF_2$ cubic interstitial sites. Subsequently, Shamu *et al.*[25] detected the infrared absorption due to these atoms at $640\pm0.5$ $cm^{-1}$. The intensity of the absorption line corresponded to an effective ionic change of 0.07.

The electronic transitions of the gadolinium $H^0$ site vanish above 100°K. This disappearance is reversible for short-term heating, and the full intensity of this site is regained upon recooling. However, conversion of $H^0$ to the original $H^-$ site takes place if the irradiated sample is left at room temperature for more than a few hours. The uv irradiated crystals have a slight violet coloration indicative of the formation of color centers. The same effect of coloration[26] and the formation of the $H^0$ gadolinium site is also obtained by x irradiation at low temperature. The recovery of the original $H^-$ site at room temperature is accompanied by quenching of the color centers. This is expected if the quenching is caused by recombination of the neutral $H^0$ atoms with extricated free electrons. Color centers in $CaF_2$ are always associated with the presence of $Y^{3+}$ and $O^{2-}$ impurities in the crystals.[27,28] The presence of yttrium in all our crystals is shown by Fig. 5, and the presence of $O^{2-}$ is proved by the characteristic emission spectrum of gadolinium $O_{2-\text{site}}$ in the hydrogenated crystals.[19]

TABLE VIII. Frequencies of local-mode vibronics observed in irradiated, hydrogenated, and deuterated crystals of calcium fluoride containing 0.05% gadolinium, recorded at 77°K.

| Impurity | Vibronic frequency ($cm^{-1}$) | Parent electronic frequency ($cm^{-1}$) | Separation ($cm^{-1}$) |
|---|---|---|---|
| $H^0$ | 31213 | 31980.4 | 767 |
| | 31302 | 32069.1 | 767 |
| | 31346 | 32113.9 | 768 |
| | ··· | 32139.7 | ··· |
| $D^0$ | 31416 | 31981.1 | 565 |
| | 31504 | 32069.1 | 565 |
| | ··· | 32114.0 | ··· |
| | ··· | 32139.9 | ··· |

## VII. ESR MEASUREMENTS

Hydrogenated and deuterated crystals of calcium fluoride containing cerium or neodymium were examined at *X* band and 4.2°K, and ESR absorption due

TABLE IX. ESR data on the various axial sites of tetragonal symmetry observed in hydrogenated and deuterated crystals of calcium fluoride containing cerium or neodymium, recorded at 4.2°K and *X* band.

| RE | Site label | Assignment | $g_{\parallel}$ | $g_{\perp}$ |
|---|---|---|---|---|
| Cerium | *A* | Fluoride-ion charge-compensated tetragonal symmetry site | $3.045\pm0.003$ | $1.384\pm0.002$ |
| | $H^-$ | Hydride-ion charge-compensated tetragonal symmetry site | $3.155\pm0.003$ | $1.333\pm0.001$ |
| | $D^-$ | Deuterium-ion charge-compensated tetragonal symmetry site | $3.160\pm0.005$ | $1.328\pm0.002$ |
| Neodymium | *A* | Fluoride-ion charge-compensated tetragonal symmetry site | $4.412\pm0.008$ | $1.301\pm0.002$ |
| | $H^-$ | Hydride-ion charge-compensated tetragonal symmetry site | $4.770\pm0.006$ | $0.980\pm0.001$ |
| | $D^-$ | Deuterium | $4.795\pm0.008$ | $0.970\pm0.002$ |

---

[22] R. G. Bessent, W. Hayes, and J. W. Hodby, Phys. Letters **15**, 115 (1965).

[23] M. Lax and E. Burstein, Phys. Rev. **97**, 39 (1955).

[24] D. W. Feldman, J. G. Castle, Jr., and J. Murphy, Phys. Rev. **138**, A1208 (1965). R. C. Newman and D. N. Chambers, in *Proceedings of the International Conference on Localized Excitations in Solids*, edited by R. F. Wallis (Plenum Press, Inc., New York, 1968), p. 520.

[25] R. E. Shamu, W. M. Hartmann, and E. L. Yasaitis, Phys. Rev. **170**, 822 (1965).

[26] J. Arends, Phys. Status Solidi **7**, 805 (1964).

[27] J. R. O'Connor and J. H. Chen, Phys. Rev. **130**, 1790 (1963).

[28] F. K. Fong and P. N. Yokom, J. Chem. Phys. **41**, 1383 (1964).

to the axial site centers was detected. The spectra are of tetragonal symmetry, and the $g$ values are given in Table IX. Similar results were also recently obtained by McLaughlan and Newman.[29] The deuterium-site $g$ values show the characteristic small shift from the hydrogen-site $g$ values.

Subsequent endor measurements on the same centers confirm the axial-site model proposed on the basis of the optical measurements. Details of the endor and ESR measurements and results will be reported elsewhere.

## VIII. SUMMARY AND CONCLUSIONS

Crystals of $CaF_2$ containing RE ions which are hydrogenated and subsequently quenched possess two hydrogenic centers exclusively characteristic of the RE impurities. One center consists of a RE-hydride pair aligned along the $\langle 100\rangle$ directions of the crystal. It is a stable impurity configuration in which the hydride ion settles as a charge compensator for the adjacent RE ion. The interaction of the two ions causes new infrared $H^-$ lines to appear. It also causes new electronic lines of the RE ion, an isotope shift in all these lines, and vibronic transitions involving the new $H^-$ local modes.

The other center is an isolated interstitial hydride ion. It can only be detected through its infrared absorption and is only observed in crystals doped with trivalent impurities. It is unstable and in crystals of low $RE^{3+}$ concentration, is converted into the former ion-pair site by slow annealing of the crystal. Irradiation of the hydrogenated crystals by uv or x rays converts the hydride negative ion into a neutral hydrogen atom, which may remain in its previous location or may wander to new sites depending on the ambient temperature. This atom is sometimes located adjacent to a RE impurity, giving rise to vibronic emission of the latter. The vibronic frequency shift is due to the local-mode frequency of the neutral hydrogen.

Due to its small mass, the hydrogen can diffuse rapidly between equivalent and nonequivalent sites. Its motion can be traced by the reversible and irreversible changes in the spectra of different sites.

## ACKNOWLEDGMENTS

We wish to express thanks to M. Foguel for growing the doped calcium-fluoride crystals, to A. Kafri for providing us with his ESR results before publication, and to M. Presland for checking lifetime measurements on the gadolinium emission lines. One of us (G.D.J.) wishes to thank the Hebrew University of Jerusalem for making his visit to the University possible.

---

[29] S. D. McLaughlan and R. C. Newman, Phys. Letters **19**, 552 (1968).

---

PHYSICAL REVIEW VOLUME 183, NUMBER 2 10 JULY 1969

# ENDOR Hyperfine Constants and Lattice Distortion of $V_K$-Type Centers[*][†]

Daniel F. Daly[‡] and Robert Lee Mieher[§]
*Department of Physics, Purdue University, Lafayette, Indiana*

(Received 25 September 1968; revised manuscript received 11 April 1969)

The magnetic hyperfine dipole-dipole interaction between $V_K$-type centers (negatively charged diatomic halide molecule-ions) and the neighboring lattice nuclei has been calculated for the $V_K$ center in LiF and NaF and the $V_{KA}$ (Li) center in NaF using the $F_2^-$ wave function of Wahl. The calculated hyperfine constants are sensitive to the relative positions of the $F_2^-$ molecule-ion and the neighboring nuclei. When the calculated hyperfine constants were compared with those measured in electron-nuclear double-resonance (ENDOR) experiments, the displacements of the nuclei surrounding the $V_K$-type centers were determined. In the vicinity of the center, the lattice contracts parallel to the axis of the molecule-ion and dilates perpendicular to this axis. The contact hyperfine interaction has been estimated and compared with the values measured in ENDOR experiments. The sign and order of magnitude of the contact hyperfine constants can be explained by assuming that the closed-shell orbitals of the molecule-ion are exchange-polarized.

## I. INTRODUCTION

The $V_K$ center was discovered by Känzig when he irradiated a KCl crystal at liquid-nitrogen temperature with x rays.[1,2] By studying its electron-spin-resonance (ESR) spectrum, he determined that this center was a $Cl_2^-$ molecule-ion oriented in a [110] direction of the cubic lattice (see Fig. 1). Subsequently the optical absorption of this center was identified by Delbecq, Smaller, and Yuster.[3]

---

[*] Supported by the Advanced Research Projects Agency at Purdue University and by the National Science Foundation under Grant Nos. NSF-GP-3385 at Columbia University and NSF-GP-4680 at Purdue University.

[†] Partially based upon a thesis submitted by D. F. Daly for the Ph.D. degree at Columbia University.

[‡] Now at Bell Telephone Laboratories, Whippany, N. J.

[§] Alfred P. Sloan Fellow.

[1] W. Känzig, Phys. Rev. **99**, 1890 (1955).

[2] T. Castner and W. Känzig, J. Phys. Chem. Solids **3**, 178 (1957).

[3] C. J. Delbecq, B. Smaller, and P. H. Yuster, Phys. Rev. **111**, 1235 (1958).